

Ionic strength dependent vesicle adsorption and phase behavior of anionic phospholipids on a gold substrate

Peer-reviewed author version

PRAMANIK, Sumit; SENECA, Senne; ETHIRAJAN, Anitha; NEUPANE, Shova; RENNER, Frank & LOSADA-PEREZ, Patricia (2016) Ionic strength dependent vesicle adsorption and phase behavior of anionic phospholipids on a gold substrate. In: Biointerphases, 11 (1).

DOI: 10.1116/1.4939596

Handle: <http://hdl.handle.net/1942/21145>

Ionic strength dependent vesicle adsorption and phase behavior of anionic phospholipids on oxidized gold

Pramanik et al., Anionic lipid vesicle adsorption and phase behavior

Sumit Kumar Pramanik, Senne Seneca, Anitha Ethirajan,
Shova Neupane, Frank Uwe Renner, Patricia Losada-Pérez*

^{a)}Institute for Materials Research IMO, Hasselt University, Wetenschapspark 1, B-3590, Diepenbeek, Belgium

^{b)}IMEC, associated lab IMOMEC, Wetenschapspark 1, 3590 Diepenbeek, Belgium

^{*}Electronic mail: patricia.losadaperez@uhasselt.be

We report on the effect of ionic strength on the formation of supported vesicle layers of anionic phospholipids DMPG and DMPS onto oxidized gold. Using quartz crystal microbalance with dissipation monitoring we show that vesicle adsorption is mainly governed by NaCl concentration, reflecting the importance of electrostatic interactions in anionic lipids, as compared to zwitterionic DMPC. At low ionic strength, low or no adsorption is observed as a result of vesicle-vesicle and vesicle-surface electrostatic repulsion. At high ionic strength, the negative charges of DMPG and DMPS are screened resulting in larger adsorption and a highly dissipative intact vesicle layer. In addition, DMPS exhibits a peculiar behavior at high ionic strength that depends on the thermal history of the layer, displaying thermally-induced adsorption and layer formation.

I. INTRODUCTION

Solid-supported lipid layers are widely used model systems to mimic the cell membrane.¹⁻³ They can be classified into supported lipid monolayers (LMs), supported lipid bilayers (SLBs), or intact vesicle layers (SVLs). Owing to their large internal volume, intact SVLs are relevant systems in immunoassay and sensor applications.^{4,5} Furthermore, the fact that they can preserve a 3D structure when adhered to a solid substrate makes them useful in biophysical studies.^{6,7} The fate of lipid vesicles when adsorbed onto a solid substrate is governed by vesicle-vesicle and vesicle-substrate interactions, with van der Waals and electrostatic interactions being the most important.⁸⁻¹⁰ In particular, the salt concentration or ionic strength is a key factor to determine the type of lipid layer formed (SLB or SVL). The effect of ionic strength has been mainly studied for zwitterionic (neutral headgroup) phospholipids on silicon dioxide and titanium dioxide using several types of surface-sensitive techniques such as quartz crystal microbalance with dissipation (QCM-D), atomic force microscopy (AFM) and ellipsometry.¹⁰⁻¹⁹ For neutral phospholipids adsorbed onto negatively charged SiO₂, several pathways of vesicle adsorption and layer formation have been identified in the absence and presence of sodium chloride (NaCl) salt. In the absence of NaCl strong vesicle-surface interactions favor a fast rupture process on the substrate. Charge screening by addition of NaCl lowers the adhesive strength between the lipids and the surface and stabilizes intact vesicles.^{13,15,16} In turn, the presence of divalent cations such as Ca²⁺ or Mg²⁺ accelerates vesicle rupture by interacting with the phosphate group.^{20,21} Despite the considerable amount of research that has been devoted to the study of the formation and stability of SVLs, the vast majority of studies are limited to neutral phospholipids at the liquid disordered phase onto SiO₂ substrates, while adsorption and formation of SLVs composed of charged phospholipids remains poorly explored and restricted to few mixtures of zwitterionic and anionic phospholipids on SiO₂.²²

Anionic phospholipids, even though they are more present in bacterial membranes, play a major role in eukaryotic cells imparting a negative surface charge for binding of various

peripheral membrane proteins.²³ 1,2-dimyristoyl-sn-glycero-3-phospho-rac-glycerol (DMPG) is the most abundant anionic phospholipid in prokaryotic cell membranes and displays a peculiar thermal phase behaviour at low ionic strength.²⁴⁻²⁸ Dimyristoylphosphatidylserine (DMPS) is in turn the major anionic phospholipid in eukaryotic membranes and it is increasingly exposed in the surface of cancer cells.²⁹⁻³¹

Here we focus on anionic or negatively charged phospholipids, namely DMPG and DMPS, onto oxidized gold. Gold is a biocompatible metal with high electrical conductivity, enhanced surface plasmon resonance and compatibility for microfabrication, characteristics that make it an interesting material for sensors.³² Specifically, we study the effect of NaCl concentration on the formation and stability of DMPG and DMPS supported vesicle layers at a temperature below their melting transition, as well as their phase behaviour, and compare them to a zwitterionic phospholipid with the same alkyl chain length, namely 1,2 dimyristoyl-sn-glycero-3-phosphocholine (DMPC). To this end, we have used quartz crystal microbalance with dissipation monitoring (QCM-D), an established surface sensitive technique to characterize vesicle adsorption kinetics and formation of SVLs or SLBs,¹⁰⁻²⁰ QCM-D was recently also used to monitor thermotropic phase transitions.³³⁻³⁶

II. EXPERIMENTAL

A. *Materials*

DMPG (sodium salt), DMPS (sodium salt) and DMPC were purchased from Avanti Polar Lipids (Alabaster, AL). Their chemical structures are depicted in Figure 1. Spectroscopic grade chloroform (assay 99.3% stabilized with about 0.6% ethanol) was obtained from Analar (Normapur). HEPES buffer (pH 7.4) consisting of 10 mM HEPES from Fisher Scientific (assay 99%) and NaCl from Sigma-Aldrich (assay $\geq 99.5\%$) was used for hydration of the dried lipids.

The used concentrations of NaCl were 0, 10, 50, 100, 150, 300, and 500 mM. The quantities of lipids were determined gravimetrically using a Sartorius balance yielding a maximal mole fraction uncertainty of ± 0.002 .

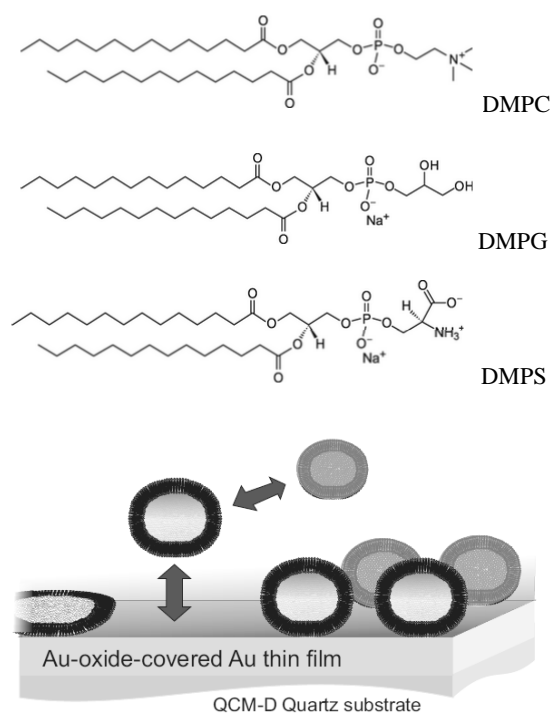


FIG. 1. Schematic chemical structure of the lipids studied in this work

B. Vesicle preparation

The lipid was first dissolved in spectroscopic grade chloroform and the solvent was evaporated under a mild flow of nitrogen in a round bottomed flask. The resulting lipid film was kept under vacuum overnight to remove residual solvent. Next, the lipid was hydrated with HEPES buffer with a given NaCl concentration. Hydration to 2 mg/ml was carried out under continuous

stirring in a temperature-controlled water bath at sufficiently high temperature (45 °C for DMPG and DMPC-containing systems and 55 °C for DMPS-containing systems, both around 20 °C above their respective main phase transition temperatures T_m). Small unilamellar vesicles (SUVs) were formed by extrusion through a filter support (Avanti Polar Lipids) with a pore size of 100 nm for 25 times. Vesicle effective sizes and polydispersities were determined by dynamic light scattering (Zeta Pals, Brookhaven Instruments Corporation). The obtained average diameters and polydispersities of the samples used are displayed in Table 1. The vesicle dispersions were stored at 4 °C and used within 2 days.

Table 1. Average diameters and polydispersities of the samples under study.

Na Cl (mM)	d (nm)	Polydispersity
DMPG		
0	107	0.30
10	121	0.26
50	93	0.28
100	129	0.15
150	108	0.12
300	134	0.05
500	119	0.09
DMPS		
0	121	0.28
10	116	0.24
50	121	0.21
100	131	0.20
150	126	0.25
300	219	0.22
300*	126	0.14
500	—	—
500*	136	0.19
DMPC		
0	118	0.03
10	122	0.03
50	125	0.05
100	119	0.04
150	123	0.06
300	134	0.06
500	134	0.09

*Measurements carried out at 50 °C

C. Quartz crystal microbalance with dissipation

Quartz crystal microbalance with dissipation monitoring (QCM-D) is an acoustic surface-sensitive technique based on the inverse piezoelectric effect. The application of an AC voltage over the sensor electrodes makes the piezoelectric quartz crystal oscillate at its acoustic resonance frequency. As a consequence, a transverse acoustic wave propagates across the crystal, reflecting back into the crystal at the surface. When the AC voltage is turned off, the oscillation amplitude decays exponentially and the frequency (f) and the energy dissipation factor (D) of different overtones are extracted.¹⁰ The dissipation D is the ratio between the dissipated energy during one vibration cycle and the total kinetic and potential energy of the crystal at that moment.

When the vesicles adsorb to an oscillating quartz crystal and eventually form an SVL, the layer is sensed as a viscoelastic hydrogel composed of the molecules and the coupled aqueous buffer. The adsorbed layer is described by a frequency-dependent complex shear modulus, defined as:³⁷

$$G = G' + iG'' = \mu_l + 2\pi i f \eta_l = \mu_l (1 + 2\pi i \chi) \quad (1)$$

where G' and G'' stand for energy storage and dissipation, respectively, f is the oscillation frequency, μ_l is the elastic shear storage modulus, η_l is the shear viscosity, and $\chi = \mu_l / \eta_l$, is the relaxation time of the layer.

For our measurements, we have used QCM-D on a Q-sense E4 instrument (Gothenborg, Sweden) monitoring the frequency and dissipation changes, Δf and ΔD . Q-sense E4 also enables heating or cooling temperature scans from 15 °C to 50 °C. AT-cut quartz crystals with Au coating (diameter 14 mm, thickness 0.3 mm, surface roughness 3 nm and resonant frequency 4.95 MHz) were used. The Au-coated quartz sensors were cleaned with a 5:1:1 mixture of Milli-Q water (conductivity of 0.055 S cm⁻¹ at 25 °C), ammonia and hydrogen peroxide, and were UV-ozone treated with a Digital PSD series UV-ozone system from Novascan for 15 min,

followed by rinsing in milli-Q water and drying with N₂. The changes in $\Delta f/n$ and in ΔD were monitored at five different overtones (from 3rd to 11th, the fundamental frequency is rather unstable since this is the one that reaches the farthest out to the edge of the sensor and may be therefore affected by the O-ring). First, a baseline with pure HEPES buffer was established and afterwards lipid vesicles were injected over the sensor chip with a flow rate of 50 $\mu\text{l}/\text{min}$. After 20 minutes the pump was switched off. Subsequent temperature scans with alternating heating and cooling were performed at rates of 0.2 $^{\circ}\text{C}/\text{min}$ and 0.4 $^{\circ}\text{C}/\text{min}$, maintaining 60 minutes of stabilization between successive ramps. The temperature stability at constant temperature was ± 0.02 $^{\circ}\text{C}$.

III. RESULTS AND DISCUSSION

A. *Vesicle adsorption and intact layer formation*

Vesicle adsorption and layer formation was carried out at 16 $^{\circ}\text{C}$, well below the melting temperature for all the studied systems. Typically for QCM-D analysis, SVL formation is characterized by decreasing $\Delta f/n$ and increasing ΔD responses reaching large plateau values with non-overlapping overtones.¹⁰ Figure 2 shows a comparison of $\Delta f/n$ and ΔD responses in the absence and presence of salt at physiological conditions of 150 mM NaCl, respectively. In the absence of salt, the kinetics of adsorption is slower than at 150 mM NaCl and the layer formed displays smaller $\Delta f/n$ and ΔD values for all three phospholipids. DMPC forms a stable SVL both in the absence and presence of salt, while the anionic phospholipids DMPG and DMPS display very small or no adsorption. For DMPS, $\Delta f/n$ and ΔD responses do not deviate from zero values during the time frame of the experiment, indicating that no DMPS vesicle

adsorption takes place. This can be understood owing to their negative charge, vesicle-vesicle and vesicle surface repulsion inhibit adsorption and layer formation. At 150 mM NaCl, surface potentials are screened and the formation of an SVL in both cases can be observed.

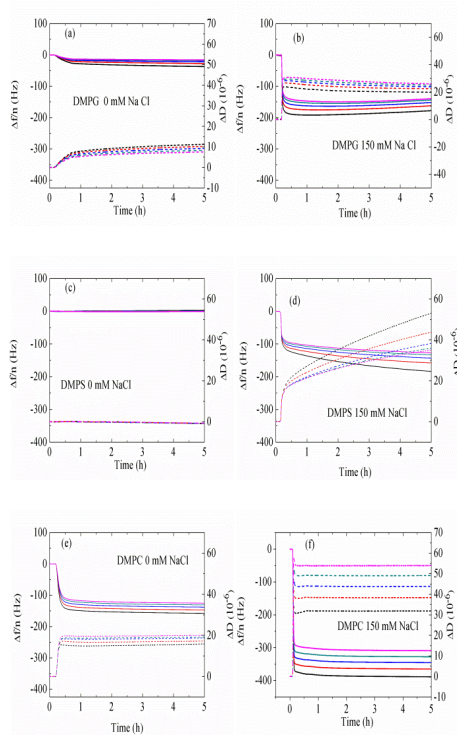


FIG 2. Time evolution of $\Delta f/n$ (solid lines) and ΔD (dashed lines) during a QCM-D experiment of vesicle adsorption at 16 °C on oxidized Au-coated quartz sensors. Black, red, blue, green and pink color correspond to the 3rd, 5th, 7th, 9th and 11th overtones, respectively.

A complete view of the ionic strength dependence of vesicle adsorption and layer formation is included in Figure 3, which depicts the $\Delta f/n$ and ΔD plateau values of overtone 7 versus the concentration of NaCl for all three systems. For DMPC two regimes can be observed, at low salt concentrations (up to 100 mM NaCl), the amount of DMPC adsorbed vesicles increases rapidly with increasing salt concentration ($\Delta f/n$ gets larger in absolute value) and the SVL

becomes more dissipative. From 100 mM NaCl onwards, $\Delta f/n$ and ΔD plateau values remain rather stable showing almost no ionic strength dependence. In the case of DMPG, $\Delta f/n$ and ΔD show a linear increase with ionic strength in the whole salt concentration range. However, the change is more gradual than in DMPC, getting almost identical $\Delta f/n$ and ΔD values for 300 mM and 500 mM NaCl, where the negative charge of DMPG is shielded by the presence of salt. At low salt concentration, DMPS shows a similar trend to DMPG until 300 mM NaCl, where a sudden change in trend is observed. Interestingly, this coincides with an increase in size as determined by DLS measurements at 25 °C. In fact, we observed that at those concentrations DMPS lipids tend to aggregate at room temperature yielding unstable vesicle dispersions. This might be related to the larger tendency of DMPS to cluster as compared to DMPG or DMPC, as recently revealed by molecular dynamics simulations.³⁸ Conversely, DLS measurements at 50 °C for 300 mM and 500 mM NaCl yield smaller sizes with lower polydispersity. As we shall see later, when performing temperature ramps, vesicle adsorption after an incubation at 50 °C yields large $\Delta f/n$ and ΔD values indicating the presence of a thermally induced effect that promotes adsorption. Specifically, the ΔD values of DMPS layers at 300 mM and 500 mM NaCl are significantly larger than the ones observed for DMPG or DMPC layer consisting of vesicles of larger size. When a vesicle layer is formed, whether it will stay intact or rather fuse to an SLB is governed by the balance between cost in curvature energy and gain in adhesion energy of the liposome to the surface. The introduction of the PS headgroup in the liposomes instead of the PG headgroup might affect this balance such that the gain in adhesion energy is not large enough to induce rupture or in our case a truncated liposome layer yielding very dissipative SVLs, as observed for liposomes adsorbed on SiO₂.²² Complementary ΔD - $\Delta f/n$ plots during the time that vesicle adsorption takes place are shown in Figure 1 of the Supplementary Information. It is worth mentioning that unlike for SiO₂ surfaces, no significant vesicle rupture event is observed under the tested experimental conditions.

Commented [L1]: I do not yet get this statement? (FR)

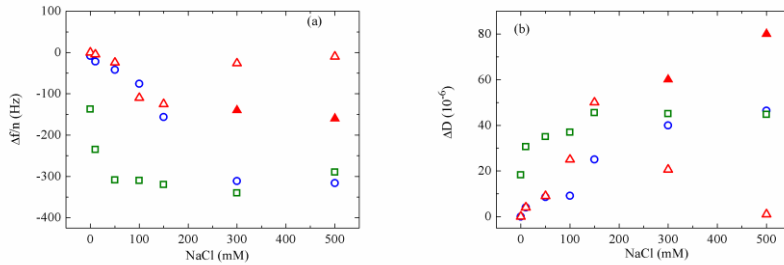


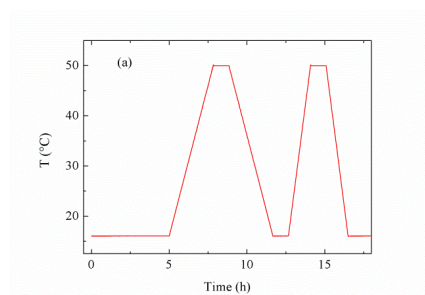
FIG. 3. Plateau values of the 7th overtone for (a) $\Delta f/n$ and (b) ΔD 5 hours after vesicle exposure at 16 °C for different concentrations of NaCl. Open blue circles refer to DMPG, open red triangles to DMPS and open green squares to DMPC. Closed red triangles denote DMPS vesicles incubated at 50 °C for 1 h.

B. Phase behavior

Once a stable layer was formed successive heating and cooling runs were performed at rates of 0.2 °C/min and 0.4 °C/min. Figure 4 shows an example of the overall experiment for 300 mM of all three lipid systems under study. Close to the main phase transition temperature both frequency and the dissipation responses deviate from the regular expected for sensors only exposed to buffer. Such anomalies reveal that structural changes are taking place and constitute a fingerprint of thermotropic phase transitions.^{32,33,35} DMPC and DMPG behave in a similar way, after the first and second heating and cooling cycles both $\Delta f/n$ and ΔD responses return back to their original SVL plateau values, indicating that the number of vesicles forming the SVL remains intact. Conversely, DMPS exhibits an anomalous response during the first heating scan. With increasing temperature $\Delta f/n$ initially increases until around 25 °C, where $\Delta f/n$ exhibits a sudden and steep decrease (mass increase) reaching a minimum and increasing back with increasing temperature. After the subsequent cooling run, the $\Delta f/n$ and ΔD plateau values at 16 °C are much larger (in absolute value) than the original ones, indicating an increase in the amount of vesicles adsorbed and the dissipation of the layer. During the second thermal cycle

at 0.4 °C/min after one hour incubation at 50 °C, the anomaly disappears and the melting transition becomes less evident. Such a peculiar behaviour is reproducible and takes place for high NaCl concentrations (see Figure 3a in the supplementary material). In a recent study, Svedhem et al. observed a peculiar behavior in the frequency and dissipation responses of DPPC vesicles. During a first heating run, $\Delta f/n$ initially decreased and later experienced a sudden and steep increase. The observed changes were ascribed to a phase transition-induced vesicle rupture.³⁹ In our case, we observe the opposite effect, a temperature-induced vesicle adsorption takes place and we relate it to the fact that DMPS displays the highest Na⁺ binding affinity of all the three phospholipids, as a result of the strong ion binding by the carboxylate group. Such an affinity might affect lipid solubility which is temperature sensitive, thus yielding a peculiar adsorption behaviour.

For the sake of comparison, we have included the $\Delta f/n$ and ΔD time responses during the subsequent heating and cooling runs for DMPS in 100 mM NaCl (see Figure 4e). Unlike higher concentrations 300 mM and 500 mM NaCl, the $\Delta f/n$ and ΔD plateau values remain rather constant denoting no significant mass adsorption nor layer dissipation upon a temperature change.



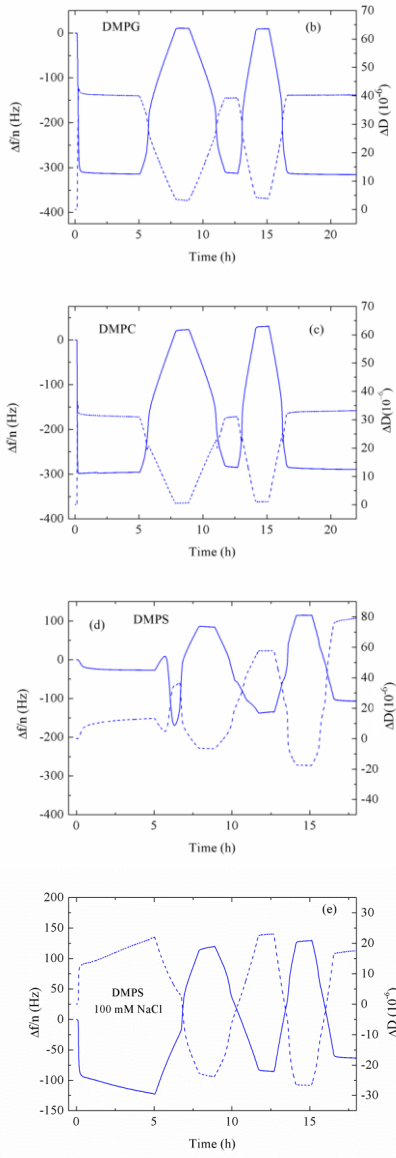


FIG. 4. (a) Temperature vs time. (b)-(d) 7th overtone $\Delta f/n$ (blue solid line) and ΔD (blue dashed line) vs time for DMPG, DMPC and DMPS vesicle layers exposed to HEPES buffer containing 300 mM NaCl and (e) DMPS vesicle layers exposed to HEPES buffer containing 100 mM NaCl.

As above mentioned, the signature of the main phase transition or melting is characterized by an anomalous behavior in the frequency and dissipation shift responses. A useful way of looking at the phase transition behavior is to plot the temperature derivative of the frequency curves making determination of the onset and completion temperatures more straightforward.³⁶ Figure 4a shows an example of Δf and its temperature derivative $(d\Delta f/n)/dT$ for DMPG and DMPC with 300 mM NaCl upon heating at 0.2 °C/min. The jump in $\Delta f/n$ corresponds to a maximum in the $(d\Delta f/n)/dT$ curve. Both DMPG and DMPC behave in the same way at high ionic strength showing a narrow, highly cooperative main transition at around 24 °C, in agreement with previous calorimetric measurements.^{26,40} Upon cooling, similar peaks are observed with a slight degree of hysteresis (~ 0.7 °C), which increases with the rate of 0.4 °C/min (see Figure 2 in the supplementary information). Figure 5b in turn shows a comparison of the thermal responses for DMPS vesicles with 300 mM NaCl buffer incubated for five hours at 16 °C and for one hour at 50 °C. Both systems show the melting transition at the expected temperature range (~ 37 °C),⁴¹ while for the system incubated at low temperature an additional feature arises. This feature is irreversible and does not take place during the second heating run. For 500 mM NaCl, the feature takes place at even higher temperatures (see Figure 3 in the supplementary material).

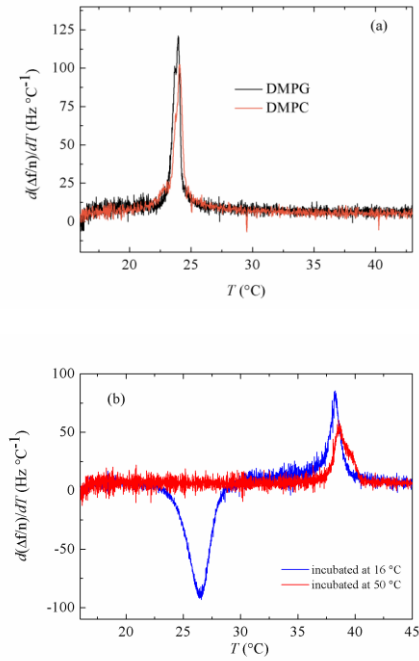
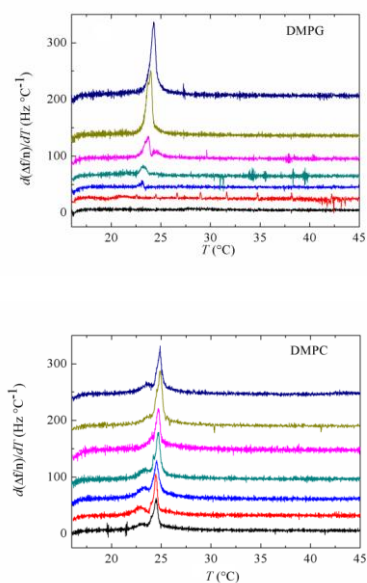


FIG. 5. (a) Temperature dependence of the first-order derivative of the frequency shift of a DMPC layer (black solid line) and DMPS layer (orange solid line) in 500 mM NaCl upon heating at 0.2 °C/min. (b) Temperature dependence upon heating of the first-order derivative of the frequency shift of a DMPS layer incubated at 16 °C (blue solid line) and at 50 °C (red solid line).

Figure 6 shows an overview of the temperature derivative $d(\Delta f/n)/dT$ for all three phospholipids at all the studied salt concentrations upon heating at 0.2 °C/min. For coherence, heating runs DMPS at 300 mM and 500 mM NaCl at 0.4 °C/min which display a single transition have been included in Figure 6. At low NaCl concentration DMPG and DMPS show very small or no adsorption at all, thus it is not possible to detect anomalies in the frequency response that account the influence of salt at those low concentrations. In turn, the zwitterionic DMPC shows a rather independent phase behaviour on ionic strength, the transition temperature (peak

maximum) is slightly shifted to higher temperatures at higher salt concentration, while the width of the transition and the size of the peak hardly change. With increasing salt concentration, intact vesicle layers of DMPG and DMPS are formed displaying maxima in the vicinity of their expected respective melting temperatures. For DMPG the amount of vesicles adsorbed increases gradually with increasing salt, this fact being reflected in the increasing size of the peak. At the highest concentration the peak is slightly shifted to higher temperatures. DMPS shows a similar pattern, however the transition temperature is significantly more shifted upwards, in agreement with calorimetric and electron spin resonance measurements.^{42,43} At pH 7.4, the DMPS headgroup displays a negative charge and the melting transition temperature increases with increasing salt concentration. Such a salt-induced increase is consistent with the Gouy-Chapman diffuse double-layer theory.⁴⁴



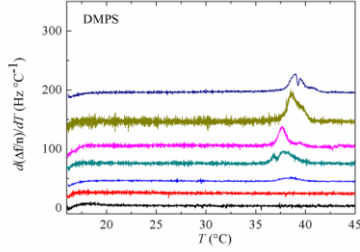


FIG. 6. Temperature profiles of the first-order temperature derivative of the frequency shifts upon heating at 0.2 °C/min. For clarity, the curves have been vertically shifted a constant amount from low to high NaCl concentration. Black, red, blue, dark cyan, pink, dark yellow and violet refer to systems in buffer with 0 mM, 10 mM, 50 mM, 100 mM, 150 mM, 300 mM, and 500 mM NaCl, respectively. For DMPS, the profiles for 300 mM, and 500 mM NaCl correspond to transitions in vesicle layers formed after incubation at 50 °C.

IV. SUMMARY AND CONCLUSIONS

We have monitored vesicle adsorption and subsequent layer formation of anionic lipids DMPG and DMPS and their thermotropic phase behavior by varying the ionic strength of the buffer solution. DMPG adsorption displays a clear trend on NaCl concentration, reflected in the linear increase of $\Delta f/n$ and ΔD plateau values upon increasing salt concentration. At high ionic strength, DMPG reaches the same $\Delta f/n$ and ΔD values as its zwitterionic counterpart DMPC, as a consequence of the PG headgroup charge screening at high ionic strength. In addition, both lipids display a similar melting profile at high ionic strength, as determined from the maxima in their temperature first-order derivative of the frequency shift. DMPS exhibits a peculiar vesicle adsorption that depends on the thermal history of the sample. In the absence of NaCl, electrostatic repulsion inhibits the adsorption of (slightly negatively charged) vesicles onto the (slightly negatively charged) oxidized gold. At intermediate ionic strengths it follows a similar behavior as DMPG, while at high ionic strength adsorption is thermally-induced, being

triggered at high temperature and precluded at low temperature, where vesicles display large average sizes. When supported vesicle layers of DMPS are formed at high temperature the expected melting transition is observed, its temperature shifting upwards with increasing ionic strength. This is most likely due to the increased screening of the charge on the phospholipid by the salt, which renders the phospholipid less soluble.

In summary, our study reflects the importance of the solution ionic strength on vesicle layer formation and stability as well as on structural transitions of negatively charged phospholipids to oxidized gold surfaces. Specifically, it shows how adsorption can be thermally activated for PS group at high ionic strengths. **in biological studies or in applications such as biosensors or membrane protein microarrays can be taken as an example of how to tune and explore adhesion of charged phospholipids also on more complex surfaces. Sensors, protein**

ACKNOWLEDGMENTS

A. E. is a FWO postdoctoral fellow. S. N., F. U. R. and P. L-P. acknowledge financial support from the FWO Odysseus program under G0D0115N project. The authors acknowledge Prof. Marlies Van Bael for the use of the DLS device.

¹E. Sackmann, *Science* **271**, 43 (1996).

²E. T. Castellana and P. S. Cremer, *Surf. Sci. Rep.* **61**, 429 (2006).

³F. Hook, B. Kasemo, M. Grunze, and S Zauscher, *ACS Nano* **2**, 2428 (2008).

⁴H. A. H. Rongen, A. Bult, and W. P. van Bennekom, *J. Immunol. Methods* **204**, 105 (1997).

⁵T. Hianik, M. Snejdarkova, L. Sokolikova, E. Meszar, R. Krivanek, V. Tvarozek, L. Novotny, and J. Wang, *Sens. Actuators B* **57**, 201 (1999).

⁶J. Salafsky, J. T. Groves, and S. G. Boxer, *Biochemistry* **35**, 14773 (1996)

- ⁷S. Heyse, T. Stora, E. Schmid, J. H. Lakey, and H. Vogel, *Biochim. Biophys. Acta* **1376**, 319 (1998).
- ⁸J. N. Israelachvili, *Intermolecular and surface forces* (Academic Press Inc, San Diego, 1985).
- ⁹P. Nollert, H. Kiefer, and F. Jahnig, *Biophys. J.* **69**, 1447 (1995).
- ¹⁰C. A. Keller and B. Kasemo, *Biophys. J.* **75**, 1397 (1998).
- ¹¹S. Sofou and J. L. Thomas, *Biosens. Bioelect.* **18**, 445 (2003).
- ¹²E. Reimhult, F. Höök, and B. Kasemo, *Langmuir* **19**, 1681 (2003).
- ¹³R. Richter, A. Mukhopadhyay, and A. Brisson, *Biophys. J.* **85**, 3035 (2003).
- ¹⁴E. Reimhult, C. Larsson, B. Kasemo, and F. Höök, *Anal. Chem.* **76**, 7211 (2004).
- ¹⁴R. Richter and A. Brisson, *Biophys. J.* **88**, 3422 (2005).
- ¹⁵B. Seantier, C. Breffa, O. Félix, and G. Decher, *J. Phys. Chem. B* **109**, 21755 (2005).
- ¹⁶S. Boudard, B. Seantier, C. Breffa, G. Decher, and O. Félix, *Thin Solid Films* **495**, 246 (2006).
- ¹⁷N. J. Cho, C. W. Frank, B. Kasemo, and F. Höök, *Nature Protocols* **5**, 1096 (2010).
- ¹⁸J. A. Jackman, J. H. Choi, V. P. Zhdanov, and N. J. Cho, *Langmuir* **29**, 11375 (2013).
- ¹⁹S. R. Tabei, J. H. Choi, G. H. Zan, V. P. Zhdanov, and N. J. Cho, *Langmuir* **30**, 10363 (2014).
- ²⁰B. Seantier and B. Kasemo, *Langmuir* **25**, 5767 (2009).
- ²¹T. Zhu, F. Xu, B. Yuang, C. Ren, Z. Jiang, Y. Ma, *Colloids Surf. B, Biointerfaces* **89**, 228 (2012).
- ²²T. Viitala, J. R. Hautala, J. Vuorinen, S. K. Wiedmer, *Langmuir* **23**, 609 (2007).
- ²³A. G. Buckland and D. C. Wilton, *Biochim. Biophys. Acta* **1483**, 199 (2000).
- ²⁴K. Lohner, *Gen. Physiol. Biophys.* **28**, 105 (2009).
- ²⁵K. A. Riske, H. G. Döbereiner, and M. T. Lamy-Freund, *J. Phys. Chem. B* **106**, 239 (2002).
- ²⁶M. T. Lamy-Freund and K. A. Riske, *Chem. Phys. Lipids* **122**, 19 (2003).
- ²⁷F. Spinozzi, L. Paccamiccio, P. Mariani, and L. Amaral, *Langmuir* **26**, 6484 (2010).
- ²⁸T. A. Enoki, V. B. Henriques, and M. T. Lamy-Freund, *Chem. Phys. Lipids* **165**, 825 (2012).

- ²⁹R. B. Gennis, *Biomembranes: Molecular Structure and Function*. (Springer-Verlag, New York, 1989).
- ³⁰S. Ran, A. Downes, and P. E. Thorpe, *Cancer Research* **62**, 6132 (2002).
- ³¹S. Riedl, B. Rinner, H. Schaider, K. Lohner, D. Zweglick, *Biometals* **27**, 981 (2014).
- ³²E. Seker, M. L. Reed, M. R. Begley, *Materials* **2**, 2188 (2009).
- ³³G. Ohlsson, A. Tigerström, F. Höök, and B. Kasemo, *Soft Matter* **7**, 10479 (2011).
- ³⁴P. Losada-Pérez, K. Jiménez-Monroy, B. van Grinsven, J. Leys, S. D. Janssens, M. Peeters, C. Glorieux, J. Thoen, K. Haenen, W. De Ceuninck, and P. Wagner, *Phys. Stat. Sol. A* **21**, 1377 (2014).
- ³⁵A. Wargenau and N. Tufenkji, *Anal. Chem.* **86**, 8017 (2014).
- ³⁶P. Losada-Pérez, M. Khorshid, D. Yongabi, and P. Wagner, *J. Phys. Chem. B* **119**, 4985 (2015).
- ³⁷N. J. Cho, K. K. Kanazawa, J. S. Glenn, C. W. Frank, *Anal. Chem.* **79**, 7027 (2007).
- ³⁸T. Broemstrup, N. Reuter, *Biophys. J.* **99**, 825 (2010).
- ³⁹Y. Ying, H. Trefna, M. Persson, B. Kasemo, S. Svedhem, *Soft Matter* **10**, 187 (2014).
- ⁴⁰S. Mabrey, J. M. Stutervant, *Proc. Natl. Acad. Sci.* **73**, 3862 (1976).
- ⁴¹R. N. A. H. Lewis, R. N. McElhany, *Biophys. J.* **79**, 2043 (2000).
- ⁴²G. Cevc, A. Watts, D. Marsh, *Biochemistry* **20**, 4955 (1981).
- ⁴³H. Hauser, G. G. Shipley, *Biochemistry* **22**, 2171 (1983).
- ⁴⁴H. Träuble, M. Teubner, P. Woolley, H. Eibl, *Biophys. Chem.* **4**, 319 (1976).